Biochemical Pharmacology 222 (2024) 116049

Contents lists available at ScienceDirect

Biochemical Pharmacology

journal homepage: www.elsevier.com/locate/biochempharm

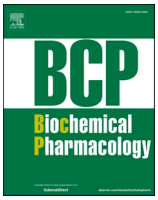

The antiangiogenic effect of digitoxin is dependent on a ROS-elicited RhoA/ROCK pathway activation

Carlotta Boscaro [b], Gudula Schimdt [c], Andrea Cignarella [b], Lucia Dal Maso [a], Chiara Bolego [a,1], Lucia Trevisi [a,*]

[a] Department of Pharmaceutical and Pharmacological Sciences, University of Padova, Padova, Italy
[b] Department of Medicine, University of Padova, Padova, Italy
[c] Institute for Experimental and Clinical Pharmacology and Toxicology, Faculty of Medicine, University of Freiburg, Freiburg, Germany

ARTICLE INFO

Keywords:
Cardiac glycosides
ROS
NADPH oxidase
RhoA GTPase
ROCK
Endothelial cell migration
Antiangiogenic drugs

ABSTRACT

We previously showed that digitoxin inhibits angiogenesis and cancer cell proliferation and migration and these effects were associated to protein tyrosine kinase 2 (FAK) inhibition. Considering the interactions between FAK and Rho GTPases regulating cell cytoskeleton and movement, we investigated the involvement of RhoA and Rac1 in the antiangiogenic effect of digitoxin. Phalloidin staining of human umbilical vein endothelial cells (HUVECs) showed the formation of stress fibers in cells treated with 10 nM digitoxin. By Rhotekin- and Pak1- pull down assays, detecting the GTP-bound form of GTPases, we observed that digitoxin (10–25 nM) induced sustained (0.5–6 h) RhoA activation with no effect on Rac1. Furthermore, inhibition of HUVEC migration and capillary-like tube formation by digitoxin was counteracted by hindering RhoA-ROCK axis with RhoA silencing or Y-27632 treatment. Digitoxin did not decrease p190RhoGAP phosphorylation at Tyr1105 (a site targeted by FAK), suggesting that RhoA activation was independent from FAK inhibition. Because increasing evidence points to a redox regulation of RhoA, we measured intracellular ROS and found that digitoxin treatment enhanced ROS levels in a concentration-dependent manner (1–25 nM). Notably, the flavoprotein inhibitor DPI or the pan-NADPH oxidase (NOX) inhibitor VAS-2870 antagonized both ROS increase and RhoA activation by digitoxin. Our results provide evidence that inhibition of HUVEC migration and tube formation by digitoxin is dependent on ROS production by endothelial NOX, which leads to the activation of RhoA/ROCK pathway. Digitoxin effects on proteins regulating cytoskeletal organization and cell motility could have a wider impact on cancer progression, beyond the antiangiogenic activity.

1. Introduction

Cardiac glycosides (CGs) are drugs of natural origin, known to be Na^+/K^+-ATPase (*i.e.* sodium pump) inhibitors. Two drugs of this class, digoxin and digitoxin, are still clinically used to treat congestive heart failure and cardiac arrhythmias. The cardiovascular effects of CGs have been associated with sodium pump inhibition, which leads to an increase of intracellular Na^+ that subsequently reduces Na/Ca exchanger activity promoting intracellular Ca^{2+} increase [1]. Besides the well-known cardiovascular effects, several preclinical and clinical studies have highlighted a potential use of CGs as anticancer drugs [2–4]. In fact, research works from several groups including our own have shown that CGs specifically block cancer cell proliferation or induce tumour cell death by mechanisms unrelated to sodium pump inhibition and calcium overload [4–6]. Early studies from Xie's group, confirmed by other laboratories, suggested that Na^+/K^+-ATPase acts as a signal transducer and that CG binding induces the activation of diverse signalling cascades and second messengers, including reactive oxygen species (ROS), that influence cell growth, survival, proliferation, and migration [7–9]. However, other targets for CGs cannot be excluded.

Abbreviations: CGs, cardiac glycosides; DCFDHDA, 2′,7′-dichlorfluorescein-diacetate; DPI, diphenyleneiodonium chloride; FAK, protein tyrosine kinase 2; FBS, fetal bovine serum; GAP, GTPase-activating protein; GEF, guanine nucleotide exchange factor; HUVECs, human umbilical vein endothelial cells; NOX, NADPH oxidase; ROCK, Rho associated coiled-coil containing protein kinase; ROS, reactive oxygen species.

* Corresponding authors at: Department of Pharmaceutical and Pharmacological Sciences, University of Padova, Largo Meneghetti 2, 35131 Padova, Italy.
E-mail address: lucia.trevisi@unipd.it (L. Trevisi).

[1] Co-last author.

https://doi.org/10.1016/j.bcp.2024.116049
Received 21 December 2023; Received in revised form 16 January 2024; Accepted 6 February 2024
Available online 9 February 2024

More recently, it has been suggested that some CGs are immunogenic cell death inducers: they promote cytotoxic effects in cancer cells while stimulating an immune response against dead-cell associated antigens [10]. On the other hand, CG use has been associated with increased risk of breast cancer due to potential estrogen-like activity [11]. Overall, the clinical relevance of CG anticancer effects appears to be controversial considering their low therapeutic index and the observation that some CGs have *in vitro* anticancer effects at concentrations not achievable in the clinical setting.

We have shown that digitoxin has a potent antiangiogenic effect against several growth factors, including pro-angiogenic agents from inflammatory cells of the tumour microenvironment [12,13]. We have also found that digitoxin inhibits ovarian cancer cell proliferation and migration induced by serum or conditioned media from human macrophages [13]. Notably, these effects have been observed at concentrations within the drug plasma therapeutic window, which is 10–40 nM [14], suggesting that digitoxin could be a suitable candidate for repositioning as an anticancer drug. Digoxin (the most clinically used CG) and digitoxin act differently on HUVECs. While digoxin at clinically relevant concentrations (0.5–2 nM) does not affect HUVEC migration and induces apoptosis at concentrations above 10 nM, digitoxin at therapeutic concentrations has an antiapoptotic effect. The molecular basis of this difference is unknown, but it is likely unrelated to the inhibition of the pumping function of Na^+/K^+-ATPase as discussed in our previous work [12].

The antimigratory and antiangiogenic effects of digitoxin have been associated with inhibition of protein tyrosine kinase 2 (FAK), a non-receptor tyrosine kinase which integrates signals from both extracellular matrix and growth factors to promote cell migration and angiogenesis [12,13,15]. Through diverse molecular connections, including those with Rho-family GTPases, FAK can influence the actin cytoskeleton to regulate cell movement [16,17].

Rho family of GTPases are members of the Ras superfamily of monomeric small (20–30 kDa) GTP-binding proteins. Rho GTPases are important regulators of cytoskeletal dynamics and other cellular processes related to the adjustment of actin cytoskeleton, including cell polarity, migration, vesicle trafficking and cytokinesis [18,19]. Within this family, Cdc42, Rac1 and RhoA are the most thoroughly characterized members. Cdc42 and Rac1 stimulate the formation of filopodia and lamellipodia, respectively, actin structures usually found at the circumference of spreading cells and the leading edge of migrating cells. On the other hand, RhoA leads to the formation of stress fibers and focal adhesions, which are involved in contractility and in maintaining a spread and adhesive phenotype of many cell types. During migration, RhoA activation promotes the formation of stress fibers at the rear of the cell and in the cell body, whose contraction enables forward movement. Moreover, it has been shown that transient RhoA activation is needed for cell migration, whereas sustained RhoA activity impedes migration [18–20].

Rho GTPases act as molecular switches of signal transduction by changing between two conformational states. In the active GTP-bound form, they interact with effector molecules and elicit a downstream response until GTP hydrolysis reverses the proteins to the inactive GDP-bound state terminating signal transduction [21]. This cycle is regulated by various groups of proteins such as guanine nucleotide exchange factors (GEFs), which induce the exchange of GDP for GTP promoting GTPase stimulation, and GTPase-activating proteins (GAPs), which catalyse the hydrolysis of GTP to GDP, thus inactivating the GTPases [19]. Moreover, Rho GTPases undergo a variety of post-translational modifications, including oxidation, that influence their localization and activity [22]. Increasing evidence points to the redox regulation of Rho GTPases, namely Rac1 and RhoA [22,23], suggesting that drugs and conditions affecting the cellular redox status could have an impact on the activity of these GTPases and, consequently, on cytoskeletal organization.

Due to the important function of Rho GTPases in controlling cell migration and considering the ability of CGs to increase intracellular ROS, we investigated the role of these proteins in the antimigratory and antiangiogenic effects of digitoxin. We show herein that digitoxin induced a persistent, ROS-dependent activation of RhoA in human umbilical vein endothelial cells (HUVECs) and that activation of RhoA/ROCK pathway is involved in the inhibition of HUVEC migration and capillary-like tube formation by digitoxin.

2. Materials and Methods

2.1. Drugs and chemicals

Cell culture reagents, digitoxin, carbonyl cyanide 4-(trifluoromethoxy) phenylhydrazone (FCCP), diphenyleneiodonium chloride (DPI), VAS 2870, and 2′,7′-dichlorfluorescein-diacetate (DCFHDA) were from Sigma-Aldrich (St. Louis, MO, USA). Collagen (rat tail) was from Roche (Basel, Switzerland). Y-27632 was purchased from Tocris Bioscience (Bristol, UK). FBS and rhodamine phalloidin were from Thermo Fisher Scientific (Waltham, MA, USA). Recombinant CNFY (*Y. pseudotuberculosis* cytotoxic necrotizing factor) was purified as previously described [24].

2.2. Human umbilical vein endothelial cells (HUVECs) isolation and culture

HUVECs were isolated in our laboratory as previously described [11] from human umbilical cords from female donors, collected after delivery from full-term normal pregnancies at the Obstetrics and Gynaecological Unit of Padua University Hospital. The donors gave their informed consent, and the collected cords were non-identifiable. The procedure was approved by the Padua University Hospital Ethics Committee (Comitato Etico per la Sperimentazione Clinica della Provincia di Padova, N.0038309, 22/06/2017). Cells were grown at 37 °C and 5 % CO_2 in complete medium: M199 supplemented with 15 % FBS, 100 μg/mL endothelial cell growth supplement (ECGS), 100 IU/mL heparin, 2 mM L-glutamine, 40 μg/mL gentamicin. HUVECs were used from passages 2 to 5.

2.3. Actin staining

HUVECs ($8x10^4$ cells/well) were seeded in 12-well plates containing glass coverslips in complete culture medium. Next day, the cells were treated with or without digitoxin for 2 h in complete cell culture medium at 37 °C. Then, cells were washed with phosphate-buffered saline (PBS), fixed with 4 % paraformaldehyde for 10 min at room temperature and permeabilized with 0.1 % Triton X-100 in PBS for 5 min. Coverslips were then washed with PBS and incubated with rhodamine-conjugated phalloidin (1 U/coverslip) for 30 min. Thereafter, coverslips were washed again in PBS and mounted with Mowiol® 4–88 (Sigma-Aldrich). Images were acquired with an LSM 800 confocal microscope (Zeiss, Oberkochen, Germany) using 20×/N.A. 0.45 air and 100×/N.A. 1.4 oil immersion objectives. Figure panels were assembled using ImageJ 1,47v (NIH, USA).

2.4. Detection of active RhoA and Rac1

Intracellular levels of active (GTP bound) RhoA and Rac1 were assessed using the Active Rho Pull-Down and Detection Kit (cat. n. 16116) and Active Rac1 Pull-Down and Detection Kit (cat. n. 16118, both Thermo Fisher Scientific), respectively, according to the manufacturer's instructions. Briefly, HUVECs ($1x10^6$ cells/dish) were seeded in 100-mm dishes in complete culture medium. After reaching confluence, cells were stimulated with digitoxin for the time and concentration indicated in Results and lysed with 400 μl of lysis buffer. The detergent-soluble supernatant was recovered after centrifugation for 15 min at 16,000 x g and 4 °C. Cell lysates were then incubated for 1 h at 4 °C with

100 µl of Glutathione Resin with GST-Rhotekin-RBD or GST-human Pak1-PBD, for detection of RhoA–GTP and Rac1–GTP, respectively. The complexes were then pelleted, washed three times, and resuspended with reducing sample buffer. After resin removal by centrifugation, the eluted samples were heated for 5 min at 95–100 °C. 25 µl/sample were used for SDS-PAGE and western blotting. 20 µg/sample of whole cell lysate were used for Western blotting analysis of the total amount of RhoA and Rac1.

2.5. RNA interference

HUVECs (3×10^5 cells/dish) were seeded into 35-mm dishes in complete medium. After 24 h, the medium was replaced and cells were transfected with Lipofectamine3000 (Invitrogen) and 20 nM siRNA ON-TARGETplus Human RhoA SMARTpool siRNAs (L-003860–00-0005, Dharmacon, Lafayette, CO, USA) per well in complete culture medium with 15 % FBS. Cells transfection with ON-TARGETplus Non-targeting Control Pool siRNA (D-001810–10-05, 20 nM Dharmacon) served as negative control. After 72 h, RhoA protein levels were measured to assess knockdown efficiency by western blotting. The effect of digitoxin on cell migration in knockdown cells for RhoA was determined by chemotaxis assay.

2.6. Chemotaxis assay

Chemotaxis experiments were performed in a 48-well modified microchemotaxis chamber (Neuro Probe, Gaithersburg, MD, USA) using 8 µm polyvinylpyrrolidine-free polycarbonate filters coated with 10 µg/ml collagen. Upper chambers were filled with 50 µl HUVEC suspension ($1.6x10^5$ cells/mL in M199 supplemented with 1 % FBS and 100 IU/mL heparin). Lower chambers were filled with complete culture medium. For assessment of basal motility, M199 supplemented with 1 % FBS and 100 IU/mL heparin was added in the lower chamber. Tested compounds (digitoxin, Y-27632) were added, as indicated in Results, both in the upper and lower compartment. After 6 h incubation at 37 °C non-migrating cells on the upper filter surface were removed by scraping. The cells migrated to the lower side of the filter were stained with Diff-Quick stain (VWR Scientific Products, Bridgeport, NJ, USA) and densitometric analysis was performed using ImageJ 1,47v. Each experimental condition was performed in sextuplicate. Results are reported as arbitrary units of O.D.

2.7. Analysis of phospho-p190RhoGAP levels

HUVECs ($3x10^5$cells/well) were seeded in 35-mm dishes in complete culture medium. The following day, fresh medium was added. After reaching confluence, the medium was replaced with M199 supplemented with 1 % FBS and 100 IU/mL heparin for 16 h. Then cells were treated with complete medium (15 % FBS) for 0.5–4 h in the presence or absence of 25 nM digitoxin (added 1 h before cell medium change). At the end of the treatment, cells were lysed and centrifugated. The supernatants were collected for SDS-PAGE and Western blotting as described below.

2.8. Western blotting

At the end of cell treatments (for analysis of phospho-p190RhoGAP levels) or siRNA transfection, cells were lysed with lysis buffer (PBS supplemented with 1.2 % Triton X-100, 1X Roche cOmpleteTM inhibitor cocktail, 2.5 mM NaF, 2 mM sodium pyrophosphate, 4 mM Na orthovanadate, 1 mM PMSF). After centrifugation at 10000 x g for 15 min, supernatants were collected and proteins quantification was performed by the BCA assay (Euroclone, Milan, Italy).

Cell lysates (20–40 µg) were separated on 10 % SDS-PAGE and transferred onto PVDF membranes (Hybond-P, Amersham, Little Chalfont, UK). Membranes were then blocked and probed for specific proteins using the following primary antibodies: rabbit anti-RhoA (2117, 1:1000 Cell Signaling Technology, Danvers, MA, USA); mouse anti-Rac1 (16118, 1:1000, Thermo Fisher Scientific); rabbit anti-phospho-p190RhoGAP Tyr 1105 (PA5-36713, 1:1000, Thermo Fisher Scientific); rabbit anti-GAPDH (ab181602 1: 10,000 Abcam, Cambridge, UK); mouse anti-β-actin (SC-47778, 1:1000, Santa Cruz Biotechnology Inc., Dallas, TX, USA). After washing, membranes were incubated with appropriate secondary HRP-conjugated antibodies (Vector Laboratories, Burlingame, CA, USA) at 1:5000 dilution. Bands were detected by chemiluminescence using the Clarity Western ECL substrate (Bio-Rad, Hercules, California, USA). Images were acquired with C400 Azure Imaging System (Azure Biosystem, Dublin, CA, USA). Densitometric analysis of the bands was performed with Image J 1,47v. Data are expressed as arbitrary units of optical density (O.D.).

2.9. Capillary–like tube formation assay

HUVECs ($8x10^3$ cells/well) were plated onto a thin layer (50 µl) of basement membrane matrix (Matrigel™, Corning Corp., Corning, NY, USA) in 96-well plates and incubated at 37 °C for 4 h in complete culture medium with digitoxin (10 nM) in the presence or absence of Y-27632 (10 µM), a selective inhibitor of Rho associated coiled-coil containing protein kinase (ROCK). One image per well was captured at 40X with a phase contrast inverted microscope (Nikon Eclipse Ti, Shinagawa, Tokyo, Japan) equipped with a digital camera. Images were analysed using Angiogenesis Analyzer, a plugin developed for the ImageJ software [25]. Data on topological parameters (number of junctions, number of meshes, and mesh area) of the capillary-like network were analysed in each well.

2.10. Time course of intracellular ROS levels

The time course of intracellular ROS accumulation in intact cells was determined using 2′,7′-dichlorfluorescein-diacetate (DCFHDA). HUVECs ($2x10^4$ cells/well) were plated in white 96-well plates (ViewPlate, Perkin Elmer, Whaltman, MA, USA) in complete medium. The following day, cells were incubated for 30 min at 37 °C with 10 µM DCFHDA in physiological salt solution (PSS, 140 mM NaCl, 5.9 mM KCl, 1.8 mM $CaCl_2$, 1.4 mM $MgCl_2{\cdot}6H_2O$, 1.2 mM NaH_2PO_4, 5.5 mM glucose, 5 mM HEPES). Cells were carefully washed with PSS with 10 % FBS and incubated in the presence or absence of digitoxin (1–25 nM) in PSS containing 10 % FBS. Fluorescence was measured (485 nm excitation and 535 nm emission) with a multilabel plate reader (Victor2, Perkin Elmer/Wallac) at 37 °C for 90 min, at 5-min intervals. Fluorescence was expressed as the percentage increase of the signal measured at time 0. Each experimental condition was performed in quadruplicate. Selected experiments were performed with diphenyleneiodonium chloride (DPI, 10 µM) or VAS2870 (10 µM); intracellular ROS produced over time was expressed as area under the curve (AUC) of DCFHDA fluorescence for each experimental condition.

2.11. Measurement of mitochondrial ROS by flow cytometry

Mitochondrial ROS were detected by labelling the cells with Mitosox (Thermo Fisher Scientific). HUVECs ($3x10^5$cells) were seeded in 35-mm dishes in complete culture medium. The following day, fresh medium was added, cells were loaded with Mitosox (5 µM, 10 min) and stimulated with digitoxin (10 nM) or FCCP (5 µM) for 60 min. At the end of treatments, cells were harvested and analysed with a FacsCanto II flow cytometer (BD Biosciences, Allschwil, Switzerland), recording at least 10,000 events for each sample. Data were analysed using the FacsDiva software (BD Biosciences). Results are expressed as geometric mean fluorescence intensity of cells.

2.12. Statistical analysis

Results are presented as mean values, with error bars representing the standard error of the mean value (SEM). Statistical analysis from at least 3 independent experiments was performed using GraphPad Prism 8 (GraphPad Software Inc., La Jolla, CA, USA). The differences between control and experimental groups were analysed by Student's *t*-test, one-way ANOVA followed by *post hoc* tests, or two-way ANOVA as detailed in the figure legends. A P value of < 0.05 was considered statistically significant.

3. Results

3.1. Digitoxin induced RhoA activation and stress fibers formation in HUVECs

To test the effect of digitoxin on HUVEC cytoskeleton, we performed phalloidin staining of actin filaments. As shown in Fig. 1A, digitoxin (10 nM) treatment for 2 h resulted in the assembly of long parallel arrays of actin stress fibers that extended throughout the cell. We observed a similar pattern of cytoskeletal organization in HUVECs treated with CNFY (*Y. pseudotuberculosis* cytotoxic necrotizing factor), a toxin known to be a strong and selective activator of RhoA [24].

We next determined the effect of digitoxin on RhoA and Rac1, whose differential spatiotemporal activation is required for cell movement. Using a Rhotekin pull-down assay, we observed that 10 nM digitoxin increased the levels of activated RhoA; the effect was detectable after 30 min and persisted after 6 h of treatment (Fig. 1B). Moreover, concentration–response experiments showed that at 2 h RhoA was already activated by 1 nM digitoxin (Fig. 1C). On the contrary, digitoxin did not affect Rac1 activity at any time and concentration assessed, as demonstrated by Pak1 pull-down assay (Fig. 1D-E). The persistent RhoA stimulation, along with the lack of Rac1 activation, are in accord with the inhibition of HUVEC migration by digitoxin previously reported by our group [12,13].

3.2. Inhibition of RhoA/ROCK pathway antagonized the effect of digitoxin on HUVEC migration and capillary-like tube formation

To assess the specific involvement of RhoA in the antimigratory effect of digitoxin, we performed some experiments in HUVECs with siRNA-mediated knockdown of RhoA. Control cells were transfected with nontargeting siRNA (scramble). As shown in Fig. 2A, siRNA transfection resulted in the efficient knockdown of the protein (-80 %).

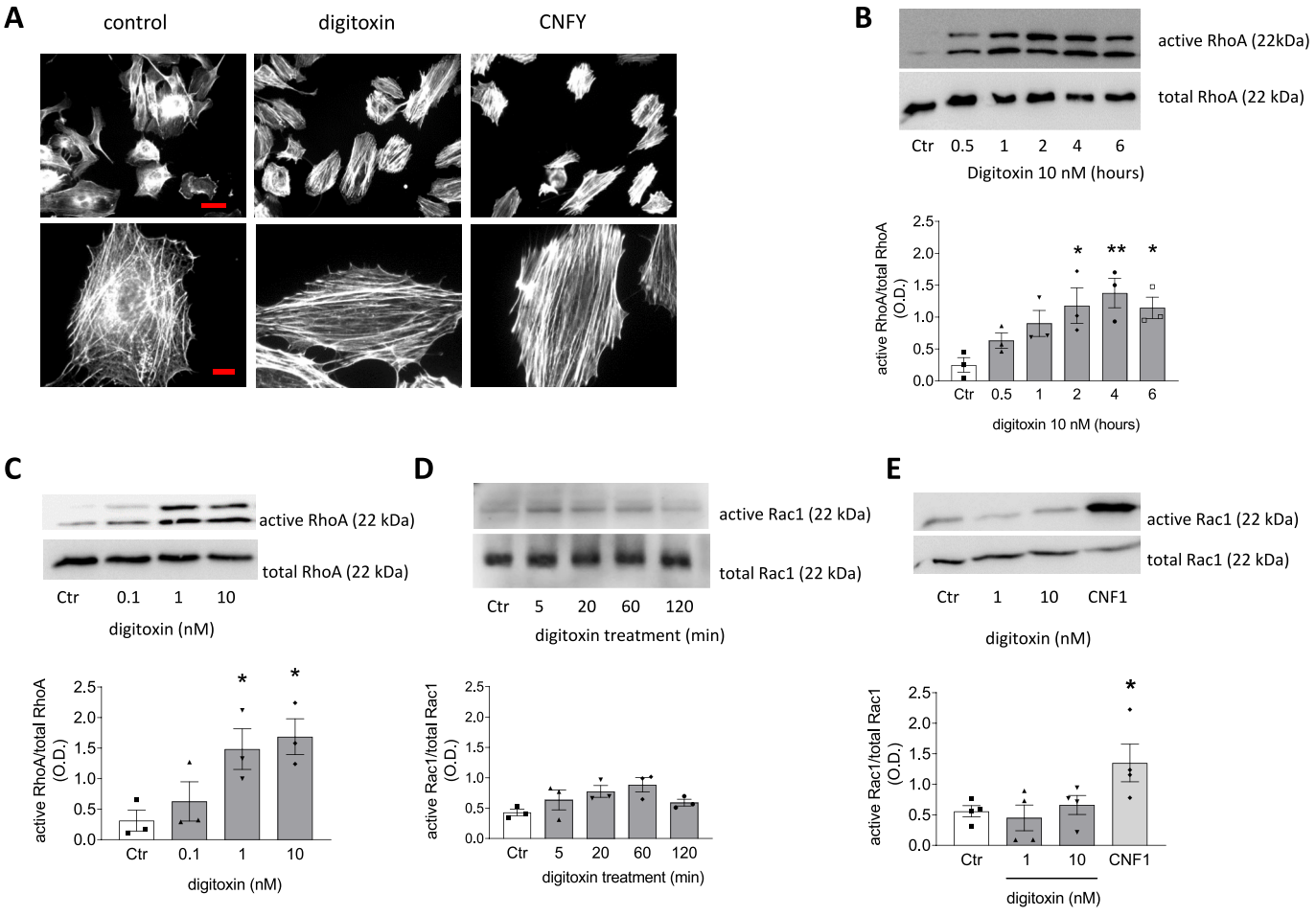

Fig. 1. Effect of digitoxin on actin organization and RhoA and Rac1 activation in HUVECs. A) Representative confocal fluorescence images showing actin staining in HUVECs. HUVECs were grown on glass coverslips in complete culture medium and treated with 10 nM digitoxin or 1 nM CNFY (*Y. pseudotuberculosis* cytotoxic necrotizing factor) for 2 h. At the end of the treatment, cells were fixed and stained with rhodamine-phalloidin as described in Methods. Upper images 20x objective (scale bar 50 μm), lower images 100x objective (scale bar 10 μm). B-E) Effect of digitoxin on RhoA and Rac1 activation in HUVECs. Cells were treated with 10 nM digitoxin in complete culture medium for the indicated time (B, D), or with 0.1–10 nM digitoxin for 2 h (C, E). Afterwards, cells were lysed and pull-down of activated RhoA or Rac1was performed as described in Methods. Upper panels: representative blots showing active and total GTPases. Lower panels: densitometric analysis of active RhoA normalized to the total amount of RhoA (B, C) or active Rac1 normalized to the total amount of Rac1 (D, E); O.D: optical density in arbitrary units, Ctr: control. Data are the mean ± SEM of n = 3 (B, C, D) or n = 4 (E), One-way ANOVA, Dunnett's post-test: *P < 0.05, **P < 0.01 (*vs* Ctr).

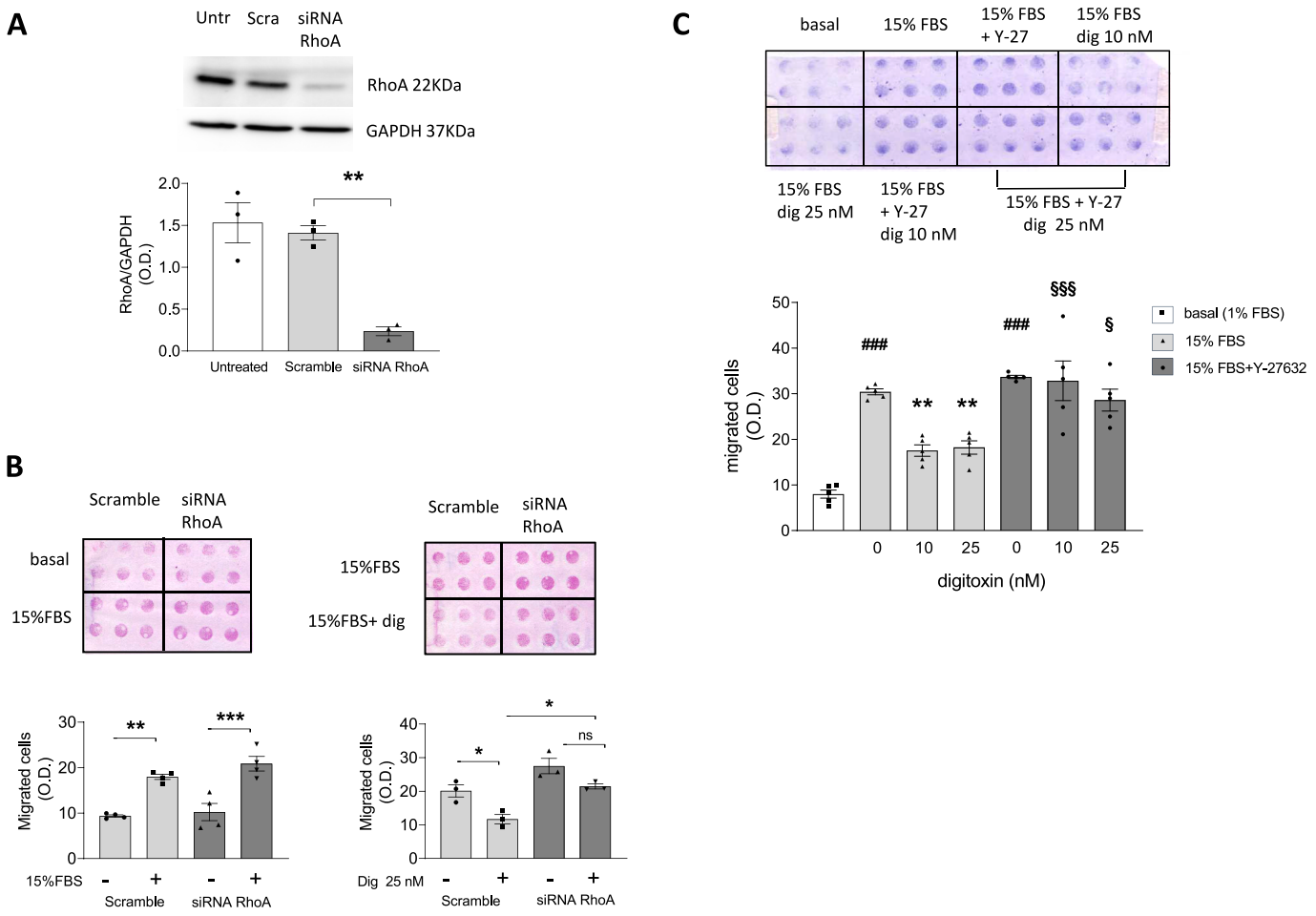

Fig. 2. Effect of RhoA silencing and ROCK inhibition on the antimigratory effect of digitoxin in HUVECs. A-B) HUVECs were transfected with 20 nM siRNA targeting RhoA or with nontargeting siRNA (scramble) for 72 h as described in Methods. Untreated: cells not transfected. A) Western blotting analysis of cell lysates was performed as described in Methods. Upper panel: representative blots of RhoA and GAPDH (loading control). Lower panel: densitometric analysis of RhoA bands, normalized to GAPDH expression; O.D: optical density in arbitrary units. Data are expressed as mean ± SEM, n = 3, One-way ANOVA, Bonferroni's post-test ** $P < 0.01$. B) Cell migration in response to complete medium (15 % FBS) was measured in RhoA knockdown cells using a microchemotaxis chamber as described in Methods. Basal: cell migration in the absence of a chemotactic gradient (1 % FBS cell medium in both upper and lower chambers). Where indicated digitoxin (25 nM) was added in both upper and lower chambers. Upper panels: representative images of a stained filters after 6 h migration. Lower panels: densitometric analysis of stained filters (O.D., optical density in arbitrary units). Data are expressed as mean ± SEM, n = 3–4. One-way ANOVA, Bonferroni's post-test, ***$P < 0.001$, ** $P < 0.01$, *$P < 0.05$, ns non-significant. C) HUVEC migration in response to complete medium (15 % FBS) was measured in a microchemotaxis chamber in the absence or presence of digitoxin (0–25 nM) as described in B. Where indicated, Y-27632 (10 μM) was added to cell culture medium. Upper panel: representative image of a stained filter after 6 h migration. Lower panel: densitometric analysis of stained filters. Data are expressed as mean ± SEM, n = 5. One-way ANOVA, Bonferroni's post- test: ### $P < 0.001$ (*vs* basal), ** $P < 0.01$ (*vs* 15 % FBS), §§§ $P < 0.001$ and § $P < 0.05$ (*vs* digitoxin alone).

Silencing of RhoA showed a non-significant increase of HUVEC migration towards a chemotactic stimulus (complete cell culture medium) (Fig. 2B). More important, digitoxin (25 nM) inhibited cell migration in control cells while in RhoA-depleted HUVECs the antimigratory effect of digitoxin was antagonized (Fig. 2B, right panels).

The serine-threonine kinase ROCK is the major effector of RhoA and participates in RhoA-induced actin organization [26]. In fact, transfecting cells with constitutively active ROCK promotes formation of stress fibers and focal adhesions, whereas truncated or kinase inactive ROCK mutants are associated with disassembly of these cytoskeletal structures [27]. To evaluate the involvement of RhoA/ROCK axis in the effect of digitoxin on HUVEC migration, we used Y-27632, a selective ROCK inhibitor [28]. As shown in Fig. 2C, digitoxin (10–25 nM) inhibited HUVEC migration toward the chemotactic stimulus, and the presence of Y-27632 (10 μM) counteracted the inhibitory effect of digitoxin on HUVEC migration.

To further analyse the involvement of ROCK in the antiangiogenic activity of digitoxin, we evaluated the effect of Y-27632 on capillary-like tube formation, an *in vitro* test that recapitulates some steps of the angiogenic process (migration and extracellular matrix degradation). As shown in Fig. 3, digitoxin (10 nM) reduced capillary-like tubes of HUVECs, expressed as number of junctions, number of meshes and total mesh area. Notably, the effect of digitoxin was antagonized by Y-27632 (10 μM).

Overall, these results suggest that the antimigratory and anti-angiogenic effects of digitoxin are dependent on the activation of the RhoA/ROCK pathway.

3.3. *Digitoxin treatment was not associated with decreased p190RhoGAP phosphorylation*

We have previously shown that inhibition of cell migration induced by digitoxin is associated with the reduction of FAK activation [12,13]. Furthermore, it has been reported that FAK phosphorylates p190RhoGAP at Tyr 1105, which enhances GAP activity, leading to RhoA inactivation [17,29]. Therefore, we explored whether digitoxin reduces p190RhoGAP phosphorylation at Tyr1105. Unexpectedly, in conditions that promoted FAK activation in HUVECs, we observed a small increase

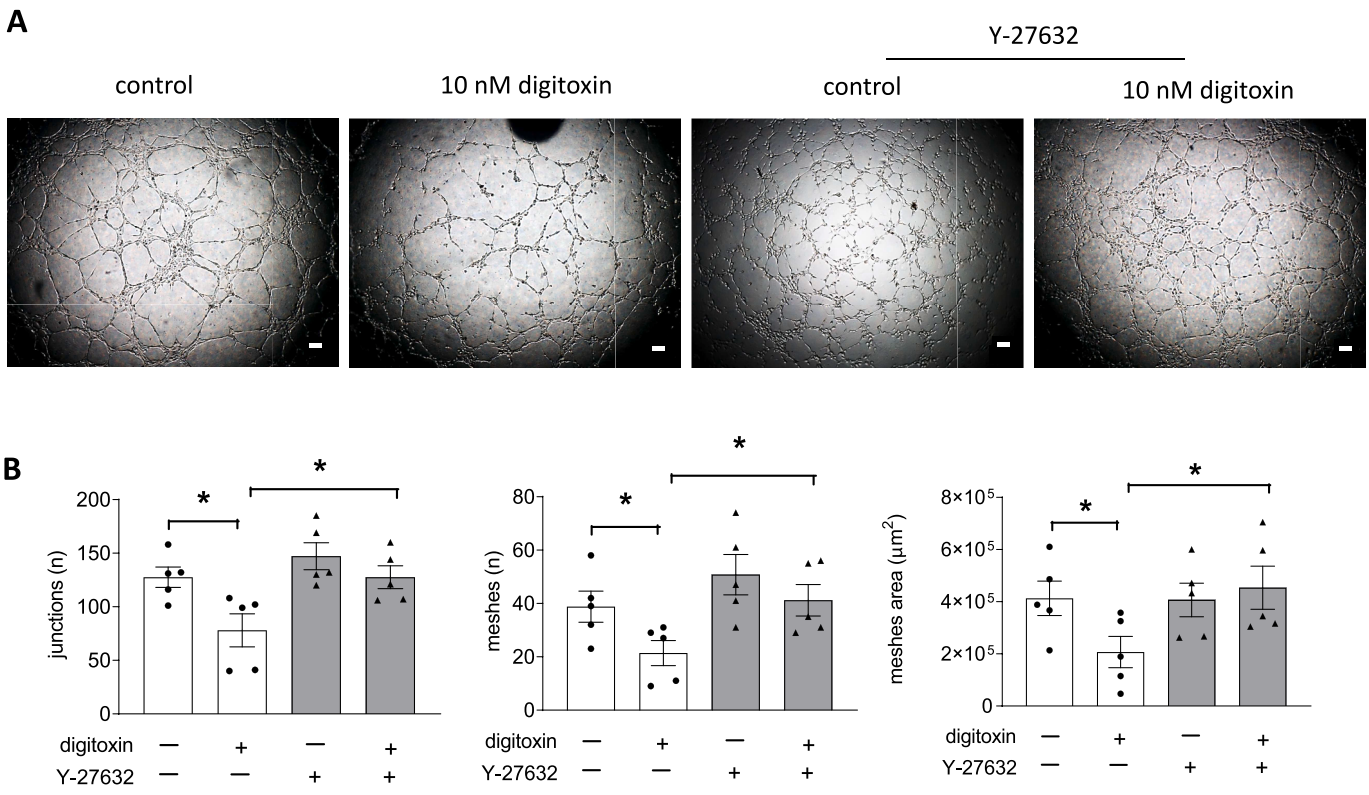

Fig. 3. Effect of digitoxin on capillary-like tube formation in the presence of the ROCK inhibitor Y-27632. HUVECs were seeded onto Matrigel-coated 96-well plates and in the absence (control) or presence of digitoxin (10 nM) for 4 h as described in Methods. Cells were treated with Y-27632 (10 μM) where indicated. A) Representative phase contrast microphotographs (scale bar: 100 μm). B) Quantitative analysis of specific parameters of capillary-like tube formation (number of meshes, number of junctions, and mesh area) as determined using Angiogenesis Analyser (ImageJ). Data are expressed as mean ± SEM, n = 5, T-test: *P < 0.05 (Df 8).

(not significant) of p190RhoGAP Tyr1105 phosphorylation that was not affected by digitoxin treatment (Fig. 4). These results suggest that mechanisms other than decreased p190RhoGAP activity are involved in RhoA activation by digitoxin.

3.4. Digitoxin increased intracellular ROS and RhoA activation by a NOX-dependent mechanism

Rho GTPases both regulate and are regulated by ROS, and evidence of either indirect or direct regulation of RhoA activation by ROS has been reported [22,23]. Moreover, we have previously shown that autophagic cell death induced by the CG ouabain in non-small cell lung cancer cells was associated with increased intracellular ROS levels [6]. However, the effect of digitoxin on ROS production and RhoA regulation in endothelial cells remains unexplored.

We first observed that HUVECs treated with digitoxin exhibited a concentration and time-dependent increase of intracellular ROS, reaching maximal levels after 1 h (Fig. 5A). To assess whether ROS produced by digitoxin were of mitochondrial origin, we performed flow cytometric analysis in HUVECs loaded with Mitosox, a selective mitochondrial superoxide indicator. Mitosox fluorescence was enhanced by the mitochondrial uncoupler FCCP but it was not affected by digitoxin treatment (10 nM for 1 h), indicating that mitochondria were not involved in digitoxin-induced ROS elevation (Fig. 5B). Conversely, pre-treatment of HUVECs with the flavoprotein inhibitor DPI (10 μM) or the pan-NOX inhibitor VAS-2870 (10 μM) [30] abolished digitoxin-induced ROS production (Fig. 5C), suggesting the involvement of NOXs in this process.

Therefore, to evaluate the role of NOXs on RhoA activation by digitoxin, we carried out pull-down experiments in HUVECs pre-treated with DPI or VAS-2870. As shown in Fig. 6, both inhibitors prevented the increase of active RhoA in digitoxin-treated cells. Collectively, these data indicate that endothelial NOX-derived ROS play a major role in RhoA activation by digitoxin.

4. Discussion

Rho family GTPases play a crucial role in the control of cell–cell and cell-extracellular matrix adhesions, as well as in cell migration, by regulating the dynamic formation and disassembly of actin filament–based structures (including lamellipodia, filopodia, invadopodia) that allow the cell to move in response to extracellular stimuli [31]. These functions of Rho GTPases are evident in endothelial cells throughout all processes involved in angiogenesis, such as vascular permeability, extracellular matrix degradation, cellular migration, proliferation, and lumen formation [32]. Furthermore, due to their involvement in migration and invasion of cancer cells, Rho GTPases could be potential targets for combined antiangiogenic and antimetastasis therapy [32,33].

In the present study, we show that digitoxin promotes RhoA activation and the formation of stress fibers in HUVECs. The persistent RhoA stimulation together with the lack of Rac1 activation are in accord with the inhibition of HUVEC migration previously observed [12]. In fact, during cell migration, a coordinated spatiotemporal activation/inactivation of different Rho GTPases is required to regulate the actin cytoskeleton organization, resulting in a forward force at the front of the cell, while adhesion forces are disrupted at the rear of the cell. Specifically, Rac1 regulates the formation of lamellipodial membrane protrusions at the front and, along with Cdc42 (which is implicated in filopodia formation), permits directional migration. On the other hand, RhoA promotes the formation of stress fibers at the rear of the cell, whose contraction enables forward movement [34,35]. Therefore, transient

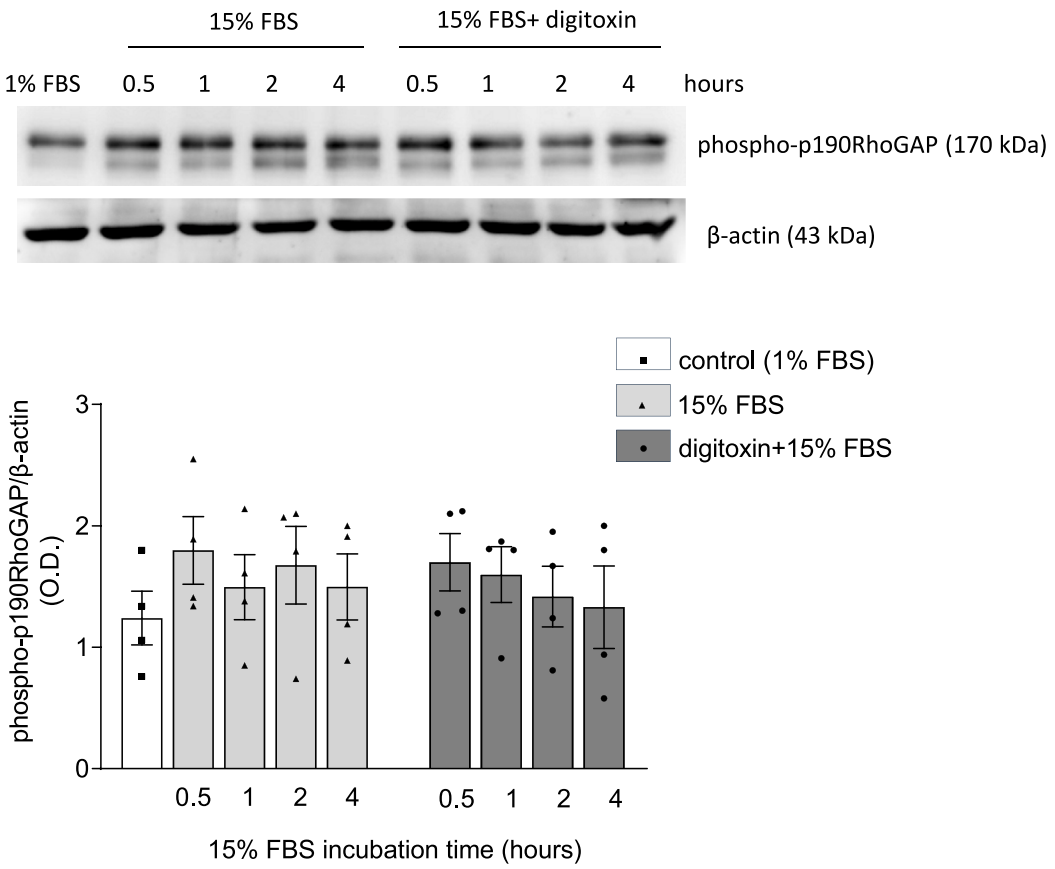

Fig. 4. Effect of digitoxin on p190RhoGAP phosphorylation. After overnight incubation with low-serum medium (1 % FBS), HUVECs were exposed to complete medium (15 % FBS) for 0.5–4 h; where indicated, the cells were treated with digitoxin (25 nM, added 1 h before cell medium change). At the end of the treatment, cells were lysed and subjected to Western blotting analysis as described in Methods. Upper panel: representative blots of phospho-p190RhoGAP Tyr1105 and beta-actin (loading control). Lower panel: densitometric analysis of the phospho-p190RhoGAP bands, normalized to beta-actin expression; O.D: optical density in arbitrary units. Data are expressed as mean ± SEM, n = 4, One-way ANOVA, Tukey's post-hoc test, non-significant.

RhoA activation is required for cell migration, whereas sustained RhoA activity impedes migration [18–20]. In line with this evidence, we observed that knockdown of RhoA antagonizes the effect of digitoxin on HUVEC migration. Furthermore, inhibition of ROCK, the main RhoA effector, with Y-27632 restores HUVEC migration and capillary-like tube formation in digitoxin-treated cells, suggesting that prolonged RhoA activation is centrally involved in the antimigratory and anti-angiogenic effects of digitoxin. Pharmacological inhibition of ROCK appears to have a higher efficacy in antagonizing the functional effects of digitoxin, especially that on tube formation. Besides RhoA, other members of the Rho subfamily such as RhoB and RhoC could activate ROCK to phosphorylate multiple downstream targets and influence endothelial barrier function and angiogenesis [36–38]. Future studies will clarify if and to what extent RhoB and Rho C contribute to the effects of digitoxin.

Previous research showed that ROCK acts as a negative regulator of VEGF-mediated angiogenesis [39]. More recently, it has been shown that increased RhoA activity has the potential to trigger antiangiogenic effects independently of ROCK [40]. In line with these studies, our findings provide the first evidence of digitoxin's ability to activate the RhoA/ROCK pathway and its consequences on endothelial function. It should be mentioned that other studies on the effects of pharmacological inhibition of ROCK reported opposite results, namely an antiangiogenic activity [41,42]. In addition, ROCK activation by CGs (ouabain, digoxin, bufalin) in HUVECs and cancer cell lines have been reported to cause cell detachment or morphological alterations associated with senescence [43–45]. These conflicting data on the functional role of ROCK could be dependent on the type of inhibitor and the concentration used, and/or the level of RhoA activation in different experimental models [46].

We have previously shown that the effects of digitoxin on cell migration were accompanied by FAK inhibition [12,13,47]. It is known that FAK negatively regulates RhoA activity via phosphorylation and activation of p190RhoGAP, which catalyses the hydrolysis of GTP to GDP and inactivates the GTPase [17,29]. Accordingly, Holinstat et al. showed that FAK phosphorylates and activates endothelial p190RhoGAP, leading to RhoA suppression, while the inhibition of FAK by the dominant negative FAK construct FRNK promotes RhoA activation and stress fibers formation [48]. For this reason, we hypothesized that stimulation of RhoA by digitoxin could be dependent on a reduction of p190RhoGAP activation. We specifically evaluated the effect of the glycoside on phospho-p190RhoGAP at Tyr1105, a phosphorylation site targeted by FAK and associated with an increase of GAP activity. Unexpectedly, we found that digitoxin did not change phospho-p190RhoGAP Tyr 1105 levels in HUVECs, thus indicating that RhoA activation and FAK inhibition in digitoxin-treated cells are two independent events. This prompted us to investigate other possible mechanisms of RhoA activation by digitoxin.

It is widely accepted that Na^+/K^+-ATPase may act as a plasma membrane receptor leading to the activation of multiple signalling pathways that are independent from its well-known pumping function [49]. Indeed, CG binding to Na^+/K^+-ATPase induce activation of diverse signalling cascades and second messengers, including ROS [7,9]. Moreover, apart from the canonical regulation of Rho GTPases activity by GEFs, GAPs and GDIs, there is increasing evidence of both indirect and direct regulation of RhoA activity by ROS [22,23]. Therefore, we explored if ROS participate in RhoA activation by digitoxin in HUVECs.

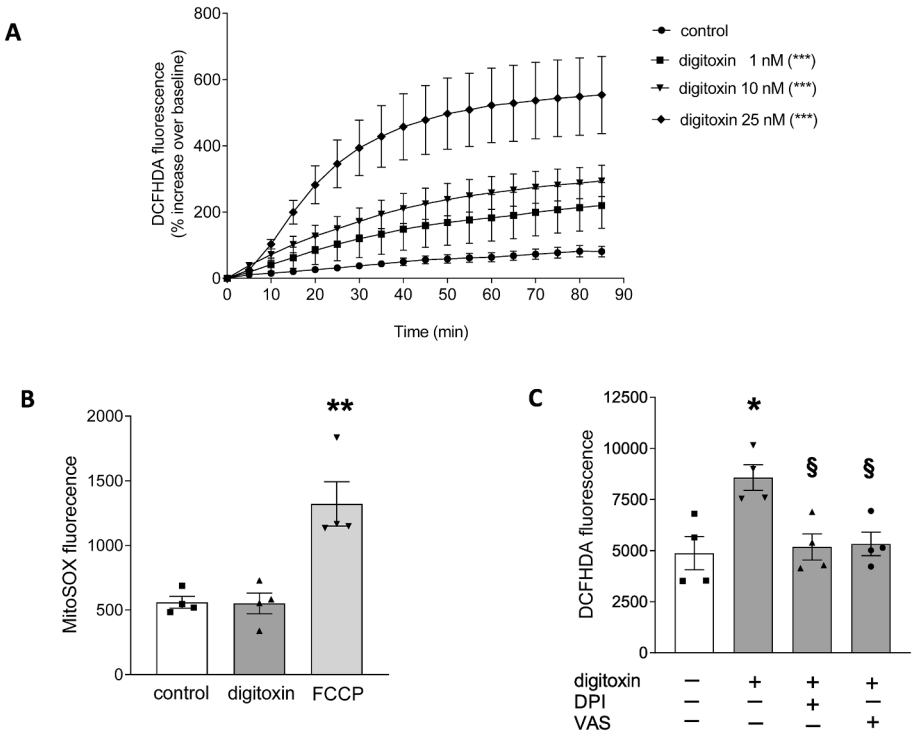

Fig. 5. Effect of digitoxin on ROS production in HUVECs. A) Time course determination of intracellular ROS in HUVECs seeded in 96-well plates, loaded with DCFHDA and treated with digitoxin (1–25 nM). Fluorescence was expressed as the percentage increase of the signal measured at time 0. Curves are plotted as means ± SEM, n = 5; significance of digitoxin treatment over time was determined by two-way ANOVA (***P < 0.001 *vs* control). B) HUVECs were seeded in 6-well plates, loaded with Mitosox for mitochondrial ROS detection and treated for 60 min with 10 nM digitoxin or 5 μM FCCP. Data are expressed as mean ± S.E.M, n = 4, **P < 0.01 (*vs* control), one-way ANOVA, Dunnett's post-test. C) Intracellular ROS accumulation was determined in HUVECs loaded with DCFHDA and treated with digitoxin (10 nM) for 90 min, in the presence of DPI (10 μM) or VAS-2870 (10 μM) added 30 min before digitoxin. Data are expressed as mean ± SEM, n = 4, One-way ANOVA, Bonferroni's post-test: *P < 0.05 (*vs* control), §P < 0.05 (*vs* digitoxin).

First, we observed that digitoxin induced a concentration-dependent increase of intracellular ROS, reaching maximal levels after 1 h of treatment. We excluded mitochondria as the source of ROS using the selective fluorescent probe Mitosox. Pioneering studies from Xie's group showed that ouabain-induced hypertrophy and contraction of rat cardiac myocytes were dependent on mitochondrial ROS [50,51], but other sites of ROS production have been described [1,52–54]. Considering that NOXs represent the major source of ROS in endothelial cells [55], we performed selected experiments in the presence of NOXs inhibitors [30] and found that the increase of ROS induced by digitoxin was abolished by pre-treatment with either the flavoprotein inhibitor DPI or the pan-NOX inhibitor VAS-2870. Notably, these inhibitors prevented the increase of active RhoA in digitoxin-treated HUVECs, thus highlighting the relevance of NOX-derived ROS as regulators of RhoA activation by digitoxin.

Vascular endothelial cells express four NOX isoforms (NOX1, NOX2, NOX4 and NOX5), but the lack of selective inhibitors impedes a pharmacological characterization of the isoform implicated in the digitoxin mechanism [55,56]. ROS production by NOX1 and NOX2 requires the association with activated Rac1 [57]; since we did not observe Rac1 stimulation during digitoxin treatment, we hypothesize that these isoforms do not contribute to RhoA activation by digitoxin. Interestingly, NOX5 is activated by Ca^{2+} increase, a relevant cellular event induced by CG binding to Na^+/K^+-ATPase [1]. Furthermore, Collado et al have demonstrated that RhoA activation triggered by angiotensin II is the consequence of NOX5-mediated ROS generation in human endothelial cells [58]. Further studies will determine the NOX isoform involved in ROS production by digitoxin and the molecular basis of the different functional effects of other CGs such as ouabain and digoxin.

Redox regulation of RhoA has been previously reported and several mechanisms pointing to either activation or inhibition of the GTPase have been described. For example, constitutively active Rac1 increases ROS levels in HeLa cells, eventually downregulating RhoA activity through a mechanism that involves the phosphorylation and activation of p190RhoGAP [59]. On the other hand, ROS could activate RhoA indirectly (namely through PKC-dependent phosphorylation and activation of p115RhoGEF) or by direct oxidation of RhoA protein, resulting in post-translational modifications [22]. In fact, biochemical studies have demonstrated that RhoA has a redox-sensitive motif, containing two cysteine residues (Cys^{16} and Cys^{20}) located directly adjacent to the phosphoryl-binding loop, and that oxidation of either residues could enhance GDP release and nucleotide exchange (GTP binding), thus increasing RhoA activity [60,61]. In accord with these findings, Aghajanian and colleagues have demonstrated that both cysteine residues of the redox-sensitive motif are essential for direct activation of RhoA by ROS in rat fibroblasts [62]. Finally, Dada et al. have shown that exogenous H_2O_2 promotes RhoA activation and stress fibers formation in lung cancer cells, and that ROS-induced RhoA/ROCK activation leads to Na^+/K^+-ATPase endocytosis [63]. Future experiments will clarify whether RhoA activation by digitoxin is mediated by ROS directly through post-translational modifications or indirectly through other redox-sensitive protein regulators of RhoA activity.

In conclusion, our results provide evidence that inhibition of HUVEC migration and capillary-like tube formation by digitoxin is dependent on ROS production by endothelial NOX, which leads to the activation of RhoA/ROCK pathway. The relevance of these findings might go beyond the inhibition of angiogenesis. By targeting proteins involved in cytoskeletal organization and cell motility, digitoxin likely prevents cancer cell invasion, overall providing a wider anticancer effect.

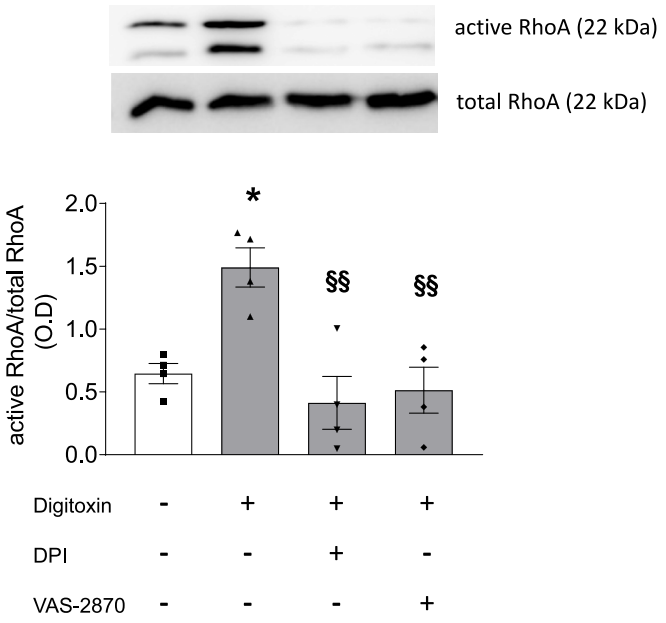

Fig. 6. Effect of NOX inhibitors on digitoxin-induced RhoA activation in HUVECs. HUVECs were treated with digitoxin (10 nM) in complete culture medium for 2 h in the presence or absence of 10 μM DPI or 10 μM VAS-2870 (added 30 min before digitoxin). At the end of the treatment, cells were lysed and pull-down of active RhoA was performed as described in Methods. Upper panel: representative blots showing active and total RhoA. Lower panel: densitometric analysis of active RhoA bands, normalized to the total amount of RhoA; O.D: optical density in arbitrary units. Data are expressed as mean ± SEM, n = 4; One-way ANOVA, Tukey's post-test: *$P < 0.05$ (*vs* control); §§ $P < 0.01$ (*vs* digitoxin).

CRediT authorship contribution statement

Carlotta Boscaro: Conceptualization, Methodology, Investigation, Formal analysis, Visualization. **Gudula Schimdt:** Conceptualization, Methodology, Investigation, Visualization. **Andrea Cignarella:** Formal analysis, Writing – review & editing, Visualization. **Lucia Dal Maso:** Investigation, Visualization. **Chiara Bolego:** Conceptualization, Methodology, Formal analysis, Visualization, Writing–review & editing. **Lucia Trevisi:** Conceptualization, Methodology, Formal analysis, Writing – original draft, Writing–review & editing, Supervision, Project administration.

Declaration of competing interest

The authors declare that they have no known competing financial interests or personal relationships that could have appeared to influence the work reported in this paper.

Data availability

Data will be made available on request.

Acknowledgments

We wish to thank Andrea Pagetta (Department of Pharmaceutical and Pharmacological Sciences, University of Padova, Padova, Italy) for technical assistance, Fabiola Modenese and the delivery room staff of the Obstetrics and Gynaecological Unit of Padova University Hospital (Padova, Italy) for the precious collaboration. This work was supported by institutional funding from the University of Padova, Padova, Italy to L.T. and Ch.B.

References

[1] M.P. Blaustein, J.M. Hamlyn, Ouabain, endogenous ouabain and ouabain-like factors: The Na+ pump/ouabain receptor, its linkage to NCX, and its myriad functions, Cell Calcium 86 (2020) 102159, https://doi.org/10.1016/j.ceca.2020.102159.
[2] E.A. Platz, S. Yegnasubramanian, J.O. Liu, C.R. Chong, J.S. Shim, S.A. Kenfield, et al., A novel two-stage, transdisciplinary study identifies digoxin as a possible drug for prostate cancer treatment, Cancer Discov. 1 (1) (2011) 68–77, https://doi.org/10.1158/2159-8274.CD-10-0020.
[3] L. Menger, E. Vacchelli, O. Kepp, A. Eggermont, E. Tartour, L. Zitvogel, et al., Trial watch: cardiac glycosides and cancer therapy, Oncoimmunology 2 (2013) e23082.
[4] R. Kumavath, S. Paul, H. Pavithran, M.K. Paul, P. Ghosh, D. Barh, V. Azevedo, Emergence of Cardiac Glycosides as Potential Drugs: Current and Future Scope for Cancer Therapeutics, Biomolecules 11 (9) (2021) 1275, https://doi.org/10.3390/biom11091275.
[5] C. Cerella, M. Dicato, M. Diederich, Assembling the puzzle of anti-cancer mechanisms triggered by cardiac glycosides, Mitochondrion 13 (2013) 225–234, https://doi.org/10.1016/j.mito.2012.06.003.
[6] A. Trenti, P. Grumati, F. Cusinato, G. Orso, P. Bonaldo, L. Trevisi, Cardiac glycoside ouabain induces autophagic cell death in non-small cell lung cancer cells via a JNK-dependent decrease of Bcl-2, Biochem. Pharmacol. 89 (2014) 197–209, https://doi.org/10.1016/j.bcp.2014.02.021.
[7] S.V. Pierre, Z. Xie, The Na, K-ATPase receptor complex: its organization and membership, Cell Biochem. Biophys. 46 (3) (2006) 303–316, https://doi.org/10.1385/cbb:46:3:303.
[8] X. Cui, Z. Xie, Protein interaction and Na+/K+-ATPase-mediated signal transduction, Molecules 22 (6) (2017) 990, https://doi.org/10.3390/molecules22060990.
[9] J. Bejček, V. Spiwok, E. Kmoníčková, S. Rimpelová, Na+/K+-ATPase Revisited: On Its Mechanism of Action, Role in Cancer, and Activity Modulation, Molecules 26 (7) (2021) 1905, https://doi.org/10.3390/molecules26071905.
[10] N.F.Z. Schneider, C. Cerella, C.M.O. Simões, M. Diederich, Anticancer and Immunogenic Properties of Cardiac Glycosides, Molecules 22 (11) (2017) 1932, https://doi.org/10.3390/molecules22111932.
[11] M.H. Osman, E. Farrag, M. Selim, M.S. Osman, A. Hasanine, A. Selim, Cardiac glycosides use and the risk and mortality of cancer; systematic review and meta-analysis of observational studies, PLoS One 12 (6) (2017) e0178611.
[12] A. Trenti, E. Zulato, L. Pasqualini, S. Indraccolo, C. Bolego, L. Trevisi, Therapeutic concentrations of digitoxin inhibit endothelial focal adhesion kinase and angiogenesis induced by different growth factors, Br. J. Pharmacol. 174 (18) (2017) 3094–3106, https://doi.org/10.1111/bph.13944.
[13] A. Trenti, C. Boscaro, S. Tedesco, A. Cignarella, L. Trevisi, C. Bolego, Effects of digitoxin on cell migration in ovarian cancer inflammatory microenvironment, Biochem. Pharmacol. 154 (2018) 414–423, https://doi.org/10.1016/j.bcp.2018.06.008.
[14] G.G. Belz, K. Breithaupt-Grögler, U. Osowski, Treatment of congestive heart failure–current status of use of digitoxin, Eur. J. Clin. Invest. 31 (Suppl 2) (2001) 10–17, https://doi.org/10.1046/j.1365-2362.2001.0310s2010.x.
[15] F.J. Sulzmaier, C. Jean, D.D. Schlaepfer, FAK in cancer: mechanistic findings and clinical applications, Nat. Rev. Cancer 14 (2014) 598–610, https://doi.org/10.1038/nrc3792.
[16] S.K. Mitra, D.A. Hanson, D.D. Schlaepfer, Focal adhesion kinase: in command and control of cell motility, Nat. Rev. Mol. Cell Biol. 6 (1) (2005) 56–68, https://doi.org/10.1038/nrm1549.
[17] A. Tomar, D.D. Schlaepfer, Focal adhesion kinase: switching between GAPs and GEFs in the regulation of cell motility, Curr. Opin. Cell Biol. 21 (5) (2009) 676–683, https://doi.org/10.1016/j.ceb.2009.05.006.
[18] M. Raftopoulou, A. Hall, Cell migration: Rho GTPases lead the way, Dev. Biol. 265 (1) (2004) 23–32, https://doi.org/10.1016/j.ydbio.2003.06.003.
[19] A.J. Ridley, Rho GTPase signalling in cell migration, Curr. Opin. Cell Biol. 36 (2015) 103–112, https://doi.org/10.1016/j.ceb.2015.08.005.
[20] V. Tkach, E. Bock, V. Berezin, The role of RhoA in the regulation of cell morphology and motility, Cell Motil. Cytoskelet. 61 (1) (2005) 21–33, https://doi.org/10.1002/cm.20062.
[21] A.L. Bishop, A. Hall, Rho GTPases and their effector proteins, Biochem. J 348 (Pt 2) (2000) 241–255.
[22] G.A. Hobbs, B. Zhou, A.D. Cox, S.L. Campbell, Rho GTPases, oxidation, and cell redox control, Small GTPases 5 (2014) e28579.
[23] M. Hurst, D.J. McGarry, M.F. Olson, Rho GTPases: Non-canonical regulation by cysteine oxidation, Bioessays 44 (2) (2022) e2100152.
[24] C. Hoffmann, M. Pop, J. Leemhuis, J. Schirmer, K. Aktories, G. Schmidt, The Yersinia pseudotuberculosis cytotoxic necrotizing factor (CNFY) selectively activates RhoA, J. Biol. Chem. 279 (16) (2004) 16026–16032, https://doi.org/10.1074/jbc.M313556200.
[25] Carpentier G, Martinelli M, Courty J, Cascone I. Angiogenesis Analyzer for ImageJ. Proceedings of the 4th ImageJ user and developer conference Luxembourg: Mondorf-les-Bains, 198–201. 2012, October 24–26.
[26] L. Julian, M.F. Olson, Rho-associated coiled-coil containing kinases (ROCK): structure, regulation, and functions, Small GTPases. 5 (2014) e29846.
[27] M. Amano, K. Chihara, K. Kimura, Y. Fukata, N. Nakamura, Y. Matsuura, K. Kaibuchi, Formation of actin stress fibers and focal adhesions enhanced by Rho-kinase, Science 275 (5304) (1997) 1308–1311, https://doi.org/10.1126/science.275.5304.1308.

[28] T. Ishizaki, M. Uehata, I. Tamechika, J. Keel, K. Nonomura, M. Maekawa, S. Narumiya, Pharmacological properties of Y-27632, a specific inhibitor of rho-associated kinases, Mol. Pharmacol. 57 (5) (2000) 976–983.
[29] W.T. Arthur, K. Burridge, RhoA inactivation by p190RhoGAP regulates cell spreading and migration by promoting membrane protrusion and polarity Mol, Biol. Cell 12 (9) (2001) 2711–2720, https://doi.org/10.1091/mbc.12.9.2711.
[30] E. Cifuentes-Pagano, G. Csanyi, P.J. Pagano, NADPH oxidase inhibitors: a decade of discovery from Nox2ds to HTS, Cell. Mol. Life Sci. 69 (14) (2012) 2315–2325, https://doi.org/10.1007/s00018-012-1009-2.
[31] C.D. Lawson, A.J. Ridley, Rho GTPase signaling complexes in cell migration and invasion, J. Cell Biol. 217 (2) (2018) 447–457, https://doi.org/10.1083/jcb.201612069.
[32] R. van der Meel, M.H. Symons, R. Kudernatsch, R.J. Kok, R.M. Schiffelers, G. Storm, et al., The VEGF/Rho GTPase signalling pathway: a promising target for anti-angiogenic/anti-invasion therapy, Drug Discov. Today 16 (5–6) (2011) 219–228, https://doi.org/10.1016/j.drudis.2011.01.005.
[33] E. Crosas-Molist, R. Samain, L. Kohlhammer, J.L. Orgaz, S.L. George, O. Maiques, et al., Rho GTPase signaling in cancer progression and dissemination, Physiol. Rev. 102 (1) (2022) 455–510, https://doi.org/10.1152/physrev.00045.2020.
[34] B.A. Bryan, P.A. D'Amore, What tangled webs they weave: Rho-GTPase control of angiogenesis, Cell. Mol. Life Sci. 64 (16) (2007) 2053–2065, https://doi.org/10.1007/s00018-007-7008-z.
[35] I. Cascone, E. Giraudo, F. Caccavari, L. Napione, E. Bertotti, J.G. Collard, et al., Temporal and spatial modulation of Rho GTPases during in vitro formation of capillary vascular network. Adherens junctions and myosin light chain as targets of Rac1 and RhoA, J. Biol. Chem. 278 (50) (2003) 50702–50713, https://doi.org/10.1074/jbc.M307234200.
[36] R. Eckenstaler, M. Hauke, R.A. Benndorf, A current overview of RhoA, RhoB, and RhoC functions in vascular biology and pathology, Biochem. Pharmacol. 206 (2022) 115321, https://doi.org/10.1016/j.bcp.2022.115321.
[37] R. Eckenstaler, A. Ripperger, M. Hauke, H. Braun, S. Ergün, E. Schwedhelm, R. A. Benndorf, Thromboxane A2 receptor activation via Gα13-RhoA/C-ROCK-LIMK2-dependent signal transduction inhibits angiogenic sprouting of human endothelial cells, Biochem. Pharmacol. 201 (2022) 115069, https://doi.org/10.1016/j.bcp.2022.115069.
[38] R. Eckenstaler, A. Ripperger, M. Hauke, M. Petermann, S.A. Hemkemeyer, E. Schwedhelm, S. Ergün, M. Frye, O. Werz, A. Koeberle, H. Braun, R.A. Benndorf, A Thromboxane A2 Receptor-Driven COX-2-Dependent Feedback Loop That Affects Endothelial Homeostasis and Angiogenesis, Arterioscler. Thromb. Vasc. Biol. 42 (4) (2022) 444–461, https://doi.org/10.1161/ATVBAHA.121.317380.
[39] J. Kroll, D. Epting, K. Kern, C.T. Dietz, Y. Feng, H.P. Hammes, et al., Inhibition of Rho-dependent kinases ROCK I/II activates VEGF-driven retinal neovascularization and sprouting angiogenesis, Am. J. Phys. Heart Circ. Phys. 296 (3) (2009) H893–H899, https://doi.org/10.1152/ajpheart.01038.2008.
[40] M. Hauke, R. Eckenstaler, A. Ripperger, A. Ender, H. Braun, R.A. Benndorf, Active RhoA Exerts an Inhibitory Effect on the Homeostasis and Angiogenic Capacity of Human Endothelial Cells, J. Am. Heart Assoc. 11 (12) (2022) e025119.
[41] B.A. Bryan, E. Dennstedt, D.C. Mitchell, T.E. Walshe, K. Noma, R. Loureiro, et al., RhoA/ROCK signaling is essential for multiple aspects of VEGF-mediated angiogenesis, FASEB J. 24 (9) (2010) 3186–3195, https://doi.org/10.1096/fj.09-145102.
[42] G.P. van Nieuw Amerongen, P. Koolwijk, A. Versteilen, V.W. van Hinsbergh, Involvement of RhoA/Rho kinase signaling in VEGF-induced endothelial cell migration and angiogenesis in vitro, Arterioscler. Thromb. Vasc. Biol. 23 (2) (2003) 211–217, https://doi.org/10.1161/01.atv.0000054198.68894.88.
[43] M. Ark, A. Ozdemir, B. Polat, Ouabain-induced apoptosis and Rho kinase: a novel caspase-2 cleavage site and fragment of Rock-2, Apoptosis 15 (12) (2010) 1494–1506, https://doi.org/10.1007/s10495-010-0529-1.
[44] A. Özdemir, Y.D. Şimay, B. İbişoğlu, B. Yaren, D. Bülbül, M. Ark, Cardiac glycoside-induced cell death and Rho/Rho kinase pathway: Implication of different regulation in cancer cell lines, Steroids 109 (2016) 29–43, https://doi.org/10.1016/j.steroids.2016.03.015.
[45] Y.D. Şimay, A. Özdemir, B. İbişoğlu, M. Ark, The connection between the cardiac glycoside-induced senescent cell morphology and Rho/Rho kinase pathway, Cytoskeleton (hoboken). 75 (11) (2018) 461–471, https://doi.org/10.1002/cm.21502.
[46] L.M. Pillay, J.J. Yano, A.E. Davis, M.G. Butler, M.O. Ezeude, J.S. Park, et al., In vivo dissection of Rhoa function in vascular development using zebrafish, Angiogenesis 25 (3) (2022) 411–434, https://doi.org/10.1007/s10456-022-09834-9.
[47] C. Baggio, C. Boscaro, F. Oliviero, L. Trevisi, G. Ramaschi, R. Ramonda, et al., Gender differences and pharmacological regulation of angiogenesis induced by synovial fluids in inflammatory arthritis, Biomed. Pharmacother. 152 (2022) 113181, https://doi.org/10.1016/j.biopha.2022.113181.
[48] M. Holinstat, N. Knezevic, M. Broman, A.M. Samarel, A.B. Malik, D. Mehta, Suppression of RhoA activity by focal adhesion kinase-induced activation of p190RhoGAP: role in regulation of endothelial permeability, J. Biol. Chem. 281 (4) (2006) 2296–2305, https://doi.org/10.1074/jbc.M511248200.
[49] A. Aperia, E.E. Akkuratov, J.M. Fontana, H. Brismar, Na+-K+-ATPase, a new class of plasma membrane receptors, Am. J. Physiol. Cell Physiol. 310 (7) (2016) C491–C495, https://doi.org/10.1152/ajpcell.00359.2015.
[50] Z. Xie, P. Kometiani, J. Liu, J. Li, J.I. Shapiro, A. Askari, Intracellular reactive oxygen species mediate the linkage of Na+/K+-ATPase to hypertrophy and its marker genes in cardiac myocytes, J. Biol. Chem. 274 (1999) 19323–19328, https://doi.org/10.1074/jbc.274.27.19323.
[51] J. Tian, J. Liu, J.I. Shapiro, K. Garlid, Z. Xie, Involvement of mitogen-activated protein kinases and reactive oxygen species in the inotropic action of ouabain on cardiac myocytes. A potential role for mitochondrial KATP channels, Mol. Cell. Biochem. (2003 242:) 181–187.
[52] Y. Yan, A.P. Shapiro, S. Haller, V. Katragadda, L. Liu, J. Tian, et al., Involvement of reactive oxygen species in a feed-forward mechanism of Na+/K+-ATPase-mediated signaling transduction, J. Biol. Chem. 288 (2013) 34249–34258, https://doi.org/10.1074/jbc.M113.461020.
[53] H.T. Ho, B. Liu, J.S. Snyder, Q. Lou, E.A. Brundage, F. Velez-Cortes, et al., Ryanodine receptor phosphorylation by oxidized CaMKII contributes to the cardiotoxic effects of cardiac glycosides, Cardiovasc. Res. 101 (1) (2014) 165–174, https://doi.org/10.1093/cvr/cvt233.
[54] H. Huang, W. Zhang, Y. Pan, Y. Gao, L. Deng, F. Li, et al., YAP Suppresses Lung Squamous Cell Carcinoma Progression via Deregulation of the DNp63-GPX2 Axis and ROS Accumulation, Cancer Res. 77 (21) (2017) 5769–5781, https://doi.org/10.1158/0008-5472.
[55] H. Wang, M.E. Hartnett, Roles of Nicotinamide Adenine Dinucleotide Phosphate (NADPH) Oxidase in Angiogenesis: Isoform-Specific Effects, Antioxidants (basel) 6 (2) (2017) 40, https://doi.org/10.3390/antiox6020040.
[56] J. Reis, M. Massari, S. Marchese, M. Ceccon, F.S. Aalbers, F. Corana, et al., A closer look into NADPH oxidase inhibitors: Validation and insight into their mechanism of action, Redox Biol. 32 (2020) 101466, https://doi.org/10.1016/j.redox.2020.101466.
[57] R.P. Brandes, N. Weissmann, K. Schröder, Nox family NADPH oxidases: Molecular mechanisms of activation, Free Radic. Biol. Med. 76 (2014) 208–226, https://doi.org/10.1016/j.freeradbiomed.2014.07.046.
[58] A. Collado, P. Marques, P. Escudero, C. Rius, E. Domingo, S. Martinez-Hervás, et al., Functional role of endothelial CXCL16/CXCR6-platelet-leucocyte axis in angiotensin II-associated metabolic disorders, Cardiovasc. Res. 114 (13) (2018) 1764–1775, https://doi.org/10.1093/cvr/cvy135.
[59] A.S. Nimnual, L.J. Taylor, D. Bar-Sagi, Redox-dependent downregulation of Rho by Rac, Nat. Cell Biol. 5 (3) (2003) 236–241, https://doi.org/10.1038/ncb938.
[60] J. Heo, S.L. Campbell, Mechanism of redox-mediated guanine nucleotide exchange on redox-active Rho GTPases, J. Biol. Chem. 280 (2005) 31003–31010, https://doi.org/10.1074/jbc.M504768200.
[61] J. Heo, K.W. Raines, V. Mocanu, S.L. Campbell, Redox regulation of RhoA, Biochemistry 45 (48) (2006) 14481–14489, https://doi.org/10.1021/bi0610101.
[62] A. Aghajanian, E.S. Wittchen, S.L. Campbell, K. Burridge, Direct activation of RhoA by reactive oxygen species requires a redox-sensitive motif, PLoS One 4 (11) (2009) e8045.
[63] L.A. Dada, E. Novoa, E. Lecuona, H. Sun, J.I. Sznajder, Role of the small GTPase RhoA in the hypoxia-induced decrease of plasma membrane Na, K-ATPase in A549 cells, J. Cell Sci. 120 (Pt 13) (2007) 2214–2222, https://doi.org/10.1242/jcs.003038.